

CRATERS OF THE SATURNIAN SATELLITE SYSTEM: I. Mimas. S.J. Robbins¹, E.B. Bierhaus², and L. Dones³. ¹LASP, 3665 Discovery Dr., University of Colorado, Boulder, CO 80303, ²Lockheed Martin Space Systems Company, PO Box 179, Mail Stop S8110, Denver, CO 80201, ³Southwest Research Institute, 1050 Walnut Street, Suite 300, Boulder, CO 80302. stuart.robbs@colorado.edu

Introduction and Background: Most young research scientists today who study large inner solar system bodies and their crater populations are spoiled: They have a plethora of image sets to choose from, uniform pixel scales in those images, repeat imagery of most areas, uniform lighting angles or variable if they choose, and established coordinate systems accurate to ~1 km or better. This is not the case with asteroids, comets, and outer solar system satellites. Especially where flyby missions are concerned (*Pioneers 10* and *11*, *Voyagers 1* and *2*, *New Horizons*), images have highly variable pixel scale over a single frame, lighting from the sun directly overhead to areas on the terminator, and poorly constrained coordinate systems. For planets that have had orbiting missions (*Galileo* at Jupiter, *Cassini* at Saturn), imaging of satellites is still flyby, and expensive fuel and a vast moon system prevent frequent passes. In this abstract, we present our approach to deriving the crater population of the Saturnian satellites in support of efforts to understand the production of non-primary (sesquinary and secondary) craters and their impact on and implications for the impacting population in the outer solar system.

Images and Processing: For this work, we identified all images of Mimas in NASA's PDS repository from *Cassini's* ISS instrument in clear or "green" filters (many pointings were almost exactly duplicated in different filters). We processed these in the USGS's *ISIS* software using standard radiometric and other corrections. All images were projected in an equirectangular system. Images that extended south of 50°S or north of 50°N were also polar projected. Despite Mimas being a triaxial ellipse [1], its approximate mean radius was used to perform the spherical projection. The final images were imported into ESRI's *ArcMap* software using a custom spheroid (*ArcMap's* built-in sphere for Mimas has its radius in decimeters instead of meters, resulting in an object 10× too large). Separate files were made for each projection.

In *ArcMap*, images were sorted by imaging sequences, where many of the images were part of a flyby and so make mosaics of certain regions at a consistent lighting angle. Within each imaging sequence, the images were sorted by pixel scale. Pixel scale as exported by *ISIS* is misleading because it is a single value, but images were very rarely taken at nadir, and so the pixel scale can vary significantly across an image. However, this was a complication we did not incorporate. Images that were not part of image sequences were simply sorted by resolution.

Because of the flyby nature of these images and lack of a uniform control network, *ISIS*-exported files show offsets from one image to the next, sometimes by

10s of kilometers. To avoid duplication of craters, we used the last publicly released basemap mosaic of Mimas as a reference and used *ArcMap's* georectify tools to manually adjust images to fit the basemap, using an average of ~75 tie points per image.

Crater Identification: Image sequences were examined as groups, and images with the highest resolution were examined first. One shapefile was used to define the area of the image that would be mapped, and the image resolution and name were saved to the polygon that defined the image. The crater counting area would ideally be the entire image with any areas that are covered by higher resolution images removed. However, because of the highly variable geometry of the image once rectified, some areas of the images were unusable for crater identification; most often this was due to cases of foreshortening.

Identification itself was done as described in [2]: A polyline shapefile was created, *ArcMap's* native streaming tools were used to create a vertex every few pixels, and the rims of craters were traced. These vertex points were saved in units of decimal degrees and exported from the shapefile. They were read into *Igor Pro* software where custom code (upgraded from [2]) finds the centroid of each traced rim, uses Great Circles to determine the distance and bearing to each point from the centroid [3], fits a best-fit circle, and saves the location and size. The image name and resolution on which the crater was identified is saved. Bierhaus is working on comparison counts to verify crater populations and techniques, similar to [4].

Due to the way these satellites were imaged, there will often be regions on satellites that – even while they were "acceptable" for crater identification on higher resolution images – are better analyzed on slightly lower resolution images taken during a different flyby / imaging sequence. As such, crater identification (and image footprint mapping) was an iterative process, requiring frequent changes and often several dozen or even hundred craters were removed in lieu of being measured on more ideal images (this process may be refined in the future to avoid this redundancy).

Results: 1. Mimas: To-date, we have completed a census of Mimantean craters on all *Cassini*-ISS images with pixel scales better than 500 m/px. This made use of 28 images; though more exist, they covered duplicate areas in worse quality. We identified 10,981 craters on these images which cover 77% of the surface area of Mimas (Fig. 1). >50% of craters with diameters $D > 1$ km were identified on images with resolutions ~250-350 m/px (Fig. 2).

Based on the shape of crater SFDs (Fig. 3), it is unlikely that our population sample over 77% of Mimas

is "complete" for craters $D < 3.5$ km. If we were to extrapolate beyond this, based on the crater population $D > 3.5$ km, we estimate there are roughly 55,000–60,000 craters $D \geq 1$ km on Mimas. Also based on Fig. 3, when accounting for resolution and image coverage limits, it appears as though the *population* (as in the size-frequency of craters) of Mimantean craters is almost uniform across the surface of the moon, with possible deviations near Herschel crater $3 < D < 10$ km where the population appears flatter than the rest of the satellite's – fewer craters at the smaller diameters in that range than otherwise expected. Proximity to Herschel and being within the continuous ejecta blanket area could account for this, where craters $D < 3$ km are back in production but those larger have not yet had time to resume a production population. We observe statistically significant crater density differences with location on Mimas, where the region around Herschel crater has fewer impacts, as would be expected.

Discussion: We are still in the early stages of this work, and at its core, it is a comparative planetology effort and so requires the populations of other satellites before we can discuss implications related to our overriding objectives. In comparison with previous work, however, this population in Fig. 3 compares well with [5] – a flat population on an R-plot for $D \geq 10$ km and decreasing for smaller diameters. It matches similar densities found by [6], and even older data based on *Voyager* images by [7]. More detailed comparisons will be done as we progress, and more quantitative comparisons will be shown at the conference.

References: [1] Thomas *et al.* (2007) doi:10.1016/j.icarus.2007.03.012. [2] Robbins & Hynke (2012) doi:10.1029/2011JE003966. [3] Vincenty (1975). [4] Robbins *et al.* (2014) doi:10.1016/j.icarus.2014.02.022. [5] Bierhaus *et al.* (2012) doi: 10.1016/j.icarus.2011.12.011. [6] Schmedemann & Neukum (2011) LPSC Abstract #2772. [7] Plescia & Boyce (1981) LPSC Abstract #428.

Funding: This work was funded by a grant from CDAPS.

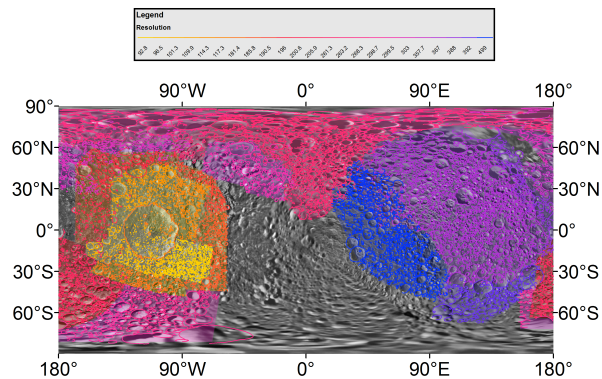


Figure 1: Mimas basemap from the ISS team, equirectangular projection. Shaded areas are image resolution footprints, and traces are actual crater rims that have been traced. Color scale is the resolution of the image based on *ISIS*.

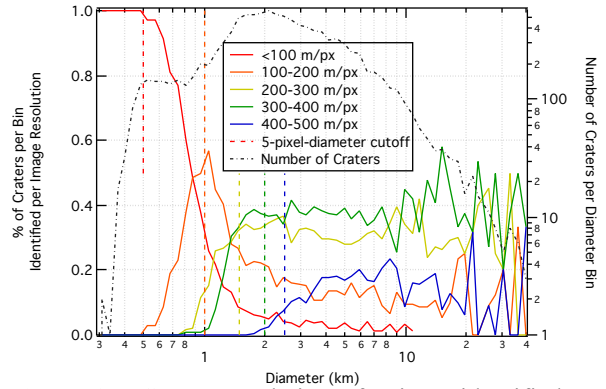


Figure 2: Crater population of Mimas identified on different image resolutions in 100 m/px intervals. Left axis corresponds to colored traces showing fraction of craters per diameter identified in that resolution range. Vertical lines are 5-px cut-offs (to the left of the line) which is a "rule of thumb," around which craters that diameter and smaller should not be identified due to inaccurate measurement and lack of completeness (demonstrated quantitatively in [4]). Right axis corresponds to dot-dash grey line and is an incremental SFD showing the number of craters identified in that diameter bin, regardless of diameter.

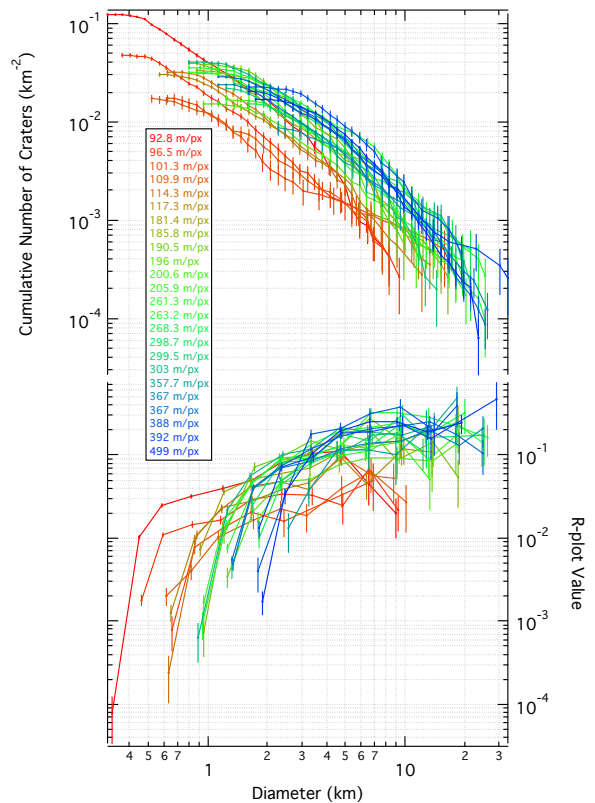


Figure 3: Normalized, stacked cumulative size-frequency distributions and R-plots of the crater populations identified at each image resolution (in all but four cases, this corresponds to individual images, as well). When excluding resolution and coverage limitations, these generally show consistent crater populations across the satellite, if varying crater densities.